MEASUREMENT OF PRESSURE FLUCTUATIONS IN TWO-DIMENSIONAL GAS-SOLID FLUIDIZED BEDS AT ELEVATED TEMPERATURES

LII-PING LEU AND CHUNG-WEN LAN
Department of Chemical Engineering, National Taiwan University, Taipei, Taiwan 10764, Republic of China

Key Words: Fluidized Bed, Pressure Fluctuations, Elevated Temperatures

Pressure fluctuations were measured in a two-dimensional gas-solid fluidized bed at temperatures ranging from 13 to 270°C. The random pressure fluctuation signals were studied on-line by the statistical method. The results indicate that the frequency spectrum, major frequency, and mean pressure amplitude depend considerably on the gas excess velocity and temperature. A probability density function of pressure fluctuations with two peaks was observed in the upper portion of the bed, indicating bubble eruption behavior at room temperature. The two peaks in the p.d.f. are transformed into a single peak at higher temperature, and the location of maximum amplitude also changes at higher temperature. Both measurements of pressure drop fluctuations and differential pressure fluctuations were used in this study, and the latter were found to be superior in the study of bubble behavior.

Introduction

In gas-solid fluidized beds, bubbles are formed when the superficial gas velocity is greater than the minimum fluidization velocity. The bubbles and the solids motion induced by them give a fluidized bed many of its important properties, such as solids mixing, heat and mass transfer and chemical conversions. Also, the gas bubbles are interrelated with pressure fluctuations around the mean pressure drop over the bed. Because

* Received August 2, 1989. Correspondence concerning this article should be addressed to L. P. Leu.

of the close relationships of pressure fluctuations and gas dynamics, these random pressure fluctuation signals are measured by two sensitive differential pressure transducers and analysed by means of statistical methods in order to investigate the behavior of fluidized beds.

The pressure drop fluctuations were studied by Kang *et al.*,[9] and Lirag and Littman.[12] They concluded that the action of bubbles causes the changes in the mode and condition of gas flow and porosity in the dense phase, and eventually induces the pressure fluctuations. Lirag and Littman concluded that the pressure fluctuations result from the bubbles escaping at the bed surface. Broadhurst and Becker[2] investigated the influence of operating conditions such as static bed height, size of bed, and kinds of particles and fluids on the slugging frequencies and amplitudes of pressure fluctuations. Similar correlations were suggested by Sadasivan *et al.*[15] Moreover, most recent research studies have been directed toward understanding the flow phenomena that cause the pressure to fluctuate [Fan *et al.*;[5] Sitnai[16]]. Some statistical analysis such as the probability density function, autocorrelation function, cross-correlation function, and spectral density function coupled with an on-line approach were used to interpret the pressure fluctuation signals.

Although most industrial fluidized beds are operated at high temperature, past works in the pressure fluctuation studies were limited to the ambient temperature. Svoboda *et al.*[18] studied the pressure fluctuations of a fluidized bed of corundum, lime, and coal ash at high temperatures up to 800°C. They found that increasing the temperature causes a decrease of the pressure fluctuation amplitudes and an increase of major frequencies at corresponding values of Uo/Umf in bubbling beds. However, effects such as measuring points, etc. on pressure fluctuations at elevated temperatures were not discussed.

The objective of this work is to explore the pressure fluctuation characteristics at elevated temperatures, such as probability density functions of pressure drop fluctuations at the bed surface, bubble rising velocities, mean amplitudes of pressure drop fluctuations and differential pressure fluctuations, and the eruption bubble frequencies in two-dimensional fluidized beds.

1. Procedure

Voltage-time signals corresponding to the pressure-time signals were sampled by an Apple-II microprocessor at a sampling rate of 100 Hz with 15,360 data points. The mean pressure difference is calculated as

$$\bar{P}=\sum_{i=1}^{N} Pi/N \tag{1}$$

The mean deviation of pressure fluctuations (or pressure fluctuation amplitude) is calculated by the following equation.

$$Y=\left(\sum_{i=1}^{N}(Pi-\bar{P})^2/(N-1)\right)^{1/2} \tag{2}$$

The dimensionless mean amplitude is defined as

$$\delta=Y/\bar{P} \tag{3}$$

The autocorrelation function is defined [Box and Jenkins[1]] as

$$Rp(\tau)=\lim_{\tau_m\to\infty}\frac{1}{\tau_m}\int_{-\tau_{m/2}}^{\tau_{m/2}} P(t)\times P(t+\tau)dt \tag{4}$$

and the cross-correlation function is defined as

$$\phi_{12}(\tau)=\lim_{\tau_m\to\infty}\frac{1}{\tau_m}\int_{-\tau_{m/2}}^{\tau_{m/2}} P1(t)\times P2(t+\tau)dt \tag{5}$$

where $P1$ is the upstream differential pressure measured at time t and $P2$ is the downstream differential pressure measured at time $t+\tau$, respectively. The average time required for a fluctuation waveform to travel between these two locations is the transit time T_{max},[6] where the cross-correlation function is maximum. The bubble rising velocity can be evaluated by an equation of Sitani:[16]

$$Ub=L/T_{max} \tag{6}$$

where L is the distance between the measuring points 1 and 2.

The power spectral density function $Gp(f)$ is represented by the Fourier transform of the autocorrelation function $Rp(\tau)$:

$$Gp(f)=2\int_{-\tau_{m/2}}^{\tau_{m/2}} Rp(\tau)\cos(2\pi f\tau)d\tau \tag{7}$$

which is calculated by the Fast Fourier Transform Algorithm [Cooly and Turkey[3]]. The frequency corresponding to the maximum power in the spectrum is considered to be the major frequency fd and other local maxima are classified as side frequencies fs in this work.

2. Experimental

A schematic diagram of the experimental apparatus is shown in **Fig. 1**. A two-dimensional $2.6\times20.8\,cm^2$ gas-solid fluidized bed equipped with a perforated distributor having 14 holes, each with a diameter of 2 mm, covered with a 200-mesh screen was used in this study. The air was regulated by an orifice flow meter and was heated by an electric heater. The temperature of the bed was measured by a K-type thermocouple. There were several pressure taps along the bed height at which the probes could easily be fixed and changed. The pressure probes were

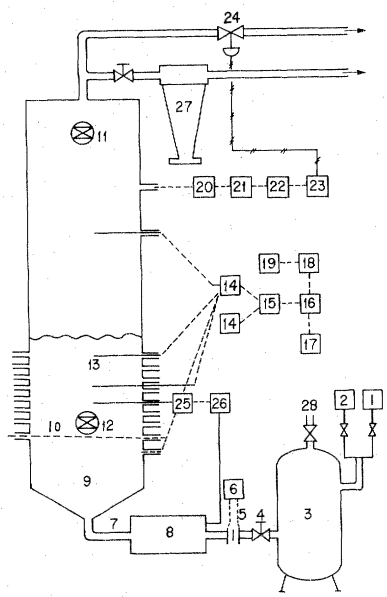

1. compressed air source
2. freon source
3. surge tank
4. valve
5. orifice meter
6. manometer
7. 1/2 in. SGP
8. heter
9. diffusion zone
10. distributor
11. particle inlet
12. particle outlet
13. pressure probe
14. pressure transducer
15. dynamic strain amplifier
16. AD/DA converter
17. 6522 VIA
18. Apple-II microprocessor
19. printer
20. pressure transducer
21. amplifier
22. controller
23. electro-pneumatic converter
24. control valve
25. thermocouple
26. temperature controller
27. cyclone separator
28. safety valve

Fig. 1. General scheme of a two-dimensional fluidized bed installation

constructed from a 1/16 inch o.d. stainless steel tube covered with a 200 mesh screen to prevent solids from penetrating into the tube. The other side of the probe was connected to a pressure transducer which was calibrated previously by using a water manometer. The data were sampled by an 8-bit A/D card with a 6522 VIA (versatile interface adaptor) as the exterior clock to set the sampling frequency. The software of sampling and data processing were written in 6502 Assembly Language. The total length of sampling time for pressure fluctuations was 128 s, and a total of 16×1024 data points were sampled.

The physical properties of materials used in this work are listed in **Table I**. Alumina and silica particles belonging to group B particles in Geldart's classification[7] were used.

3. Results and Discussion

3.1 Minimum fluidization velocities

The minimum fluidization velocities were determined by the pressure drop method[4] and the pressure fluctuation method.[14] A comparison of these measured values and values estimated by Wen and Yu's correlation[20] is shown in **Table II**. The minimum fluidization velocities at various temperatures are shown in **Fig. 2**. It can be seen that the minimum fluidization velocity decreases as the temperature increases. These tendencies were verified by the Ergun equation in the viscous region ($Re_{m_f} < 20$), and a linear relationship between the minimum fluidization velocity and 1/viscosity was observed in our study and is shown elsewhere.[11]

The minimum fluidization velocity of silica particles is much lower than the estimated values. This may be due to an inaccurate estimate of shape factor and porosity.

Table 1. Physical properties of solid particles

Material	*sp. gr.*	*εmf*	*dp* (micron)
Alumina (Al_2O_3)	3.86	0.55	290
Silica (SiO_2)	2.64	0.55	290 & 423

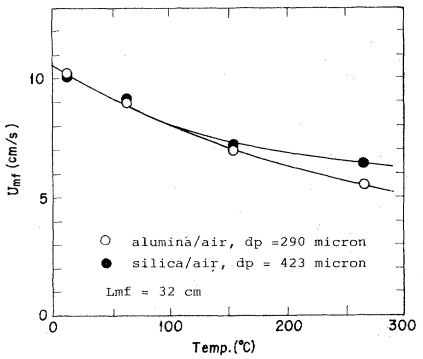

Fig. 2. Minimum fluidization velocities at various temperatures

3.2 The probability density function (p.d.f.)[5] of pressure fluctuations

The pressure drop measurement and differential pressure measurement arrangements shown in **Fig. 3** were used here. The location of the measuring points is important in interpreting the signals.[16]

Usually these two measurements have different meanings in regard to system behavior. From Sitani[16] the pressure drop fluctuations are mainly from bubble eruption; indeed both bubble eruption and bubble movement can be the main source of pressure fluc-

tuations.

Two special peaks of the p.d.f. of pressure fluctuations were measured at the bed surface at ambient temperature. The quantitative result is shown in **Fig. 4**. Obviously there are two levels of pressure as a bubble approaches and escapes from the bed surface.

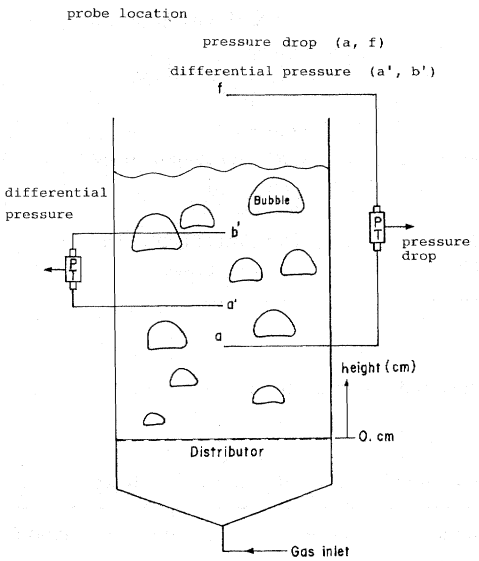

Fig. 3. Pressure probe arrangements of pressure drop measurement and differential pressure measurement

If the flow rate increases, the side peak will become higher because of the larger eruption bubble size. When the measuring point becomes lower, the mean pressure drop will increase. Relatively, the pressure drop fluctuations are more smooth due to the compromise of local porosity change and bubble eruption. However, according to Broadhurst and Becker[2] the eruption bubbles are always the main source of pressure fluctuations.

Fan *et al.*[5] measured the local pressure drop fluctuations in a three-dimensional fluidized bed and found that the shape of the p.d.f. of pressure drop fluctuations would skew to the right (the skewness is negative) in the upper portion of the bed. Their result is similar to ours at lower flow rate, but no splitting p.d.f. was found in Fan's paper. The reason for the splitting p.d.f. may be the discontinuous pressure at the moment of bubble eruption at the bed surface. At lower flow rate, the bubble size is small and the discontinuity of pressure is not obvious. At higher flow rate the bed expansion becomes large, and the pressure drop at the bubble eruption becomes smaller to depress the bed surface, as does the discontinuity of pressure.

As shown in **Fig. 5**, these two p.d.f. peaks are not observed at elevated temperatures at the same flow

Table 2. Comparison of *Umf* by pressure drop method, pressure fluctuation method, and estimated value

System	*dp* (micron)	Temp. (°C)	Press. (atm)	*Umf* by press. drop (cm/s)	*Umf* by press. fluctuations (cm/s)	*Umf* estimated by Wen and Yu correlation (cm/s)
Sand/freon	400	20	2.5	14.0	14.5	13.0
Sand/air	400	20	1	17.0	17.0	16.0
Alumina/air	290	20	1	10.0	10.0	12.7
Alumina/air	290	70	1	9.2	9.0	11.0
Alumina/air	290	170	1	7.0	7.0	8.5
Alumina/air	290	270	1	6.5	6.5	7.2
Silica/air	423	20	1	10.5	10.0	17.0
Silica/air	423	70	1	9.0	9.0	15.0
Silica/air	423	170	1	7.0	7.5	12.8
Silica/air	423	270	1	5.5	5.0	9.0
Silica/air	290	20	1	5.0	4.5	7.6

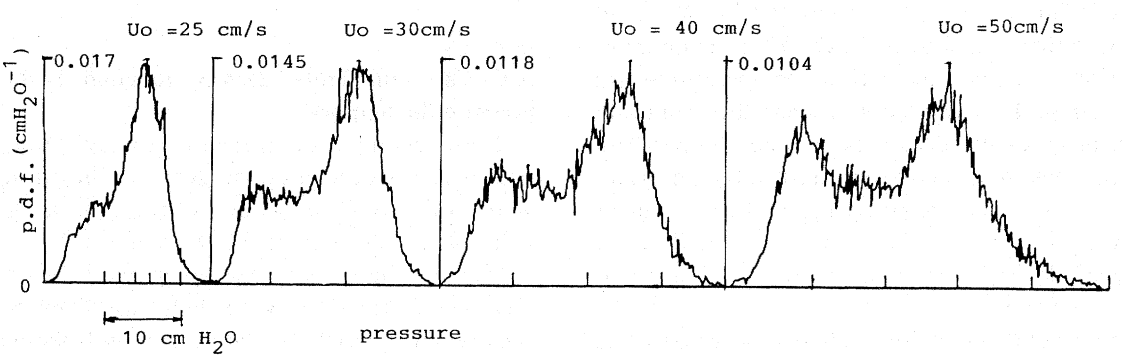

Fig. 4. Formation of two p.d.f. peaks of pressure drop fluctuations at ambient temperature for alumina/air system at $T = 13$°C. One probe is 30 cm above the distributor and the other is in the freeboard

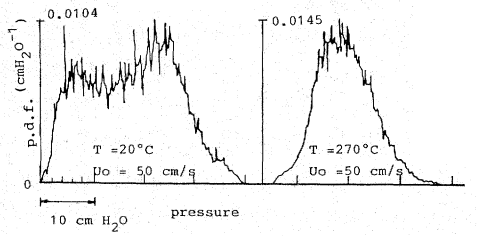

Fig. 5. Comparison of p.d.f. of pressure drop fluctuations at ambient and elevated temperature for silica/air system

rate, because of smaller bubble size and smoother pressure fluctuations, and the above observation may be indirect evidence of smaller bubble and higher fluidization quality at elevated temperatures.

3.3 Pressure fluctuations at different locations

In **Fig. 6**, the occurrence of maximum amplitudes is observed in the middle part of the bed when silica particles were used at ambient temperature. However, in **Fig. 7** the same tendency is not observed when alumina particles were used at ambient temperature. In Figs. 6 and 7 the amplitudes at elevated temperatures are also shown, but no maximum of amplitudes can be found. It was also detected by Fan *et al.*[5] and Svoboda *et al.*[18] that the magnitude of amplitude at ambient temperature increased and then decreased with the distance above the distributor. In our work, the location of maximum amplitude will shift in accordance with flow rates and temperatures. Nevertheless, it is hard to describe the behavior of the pressure fluctuation signals quantitatively at different measuring points. Any correlation would be ambiguous at different measuring locations in a broader range of operating conditions.

3.4 Influence of temperature on the bubble rising velocities

The bubble rising velocities are evaluated from cross-correlation of two signals of differential pressure fluctuations. The results at various temperatures are shown in **Fig. 8**. From Davidson and Harrison's model,[4] the free bubble rising velocity is much less than $(Uo-Umf)$ at higher rate; therefore the bubble duration time would not change significantly at elevated temperature, especially at higher flow rates. If we use two pressure drop fluctuations to evaluate the bubble rising velocity, the results obtained are questionable. We usually obtained a value several times higher than the observed one, and the reproducibility is very bad, although Fan *et al.*[6] measured the velocity of fluctuation waveform by this method. It can be seen that if there is only one bubble passing through the same cross section each time, the results of the two measurements will be similar. Moreover, if there are more than one bubble passing through the cross section each time, Fan's method cannot produce reasonable results. On the contrary,

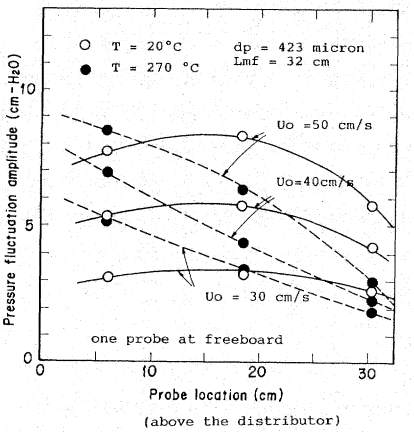

Fig. 6. Pressure drop fluctuation amplitude at various heights for silica/air system

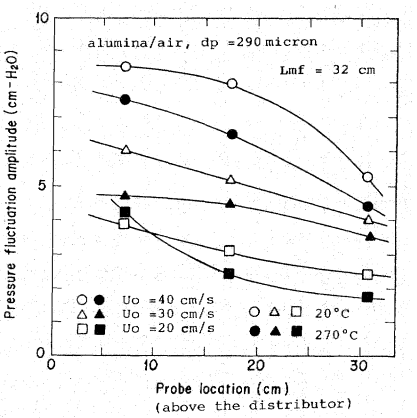

Fig. 7. Pressure drop fluctuations amplitude at various heights for alumina/air system

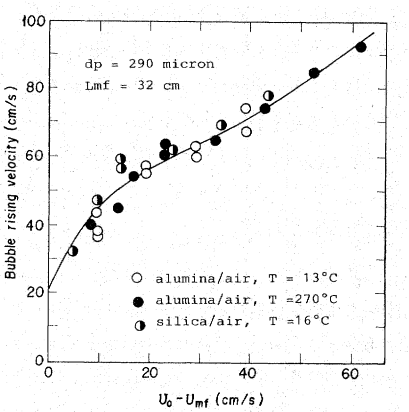

Fig. 8. Bubble rising velocity v.s. $Uo-Umf$ at various temperatures

as the differential pressure signals represent the local bubble properties,[11] the bubble rising velocity evaluated by the two differential pressure signals shows more reasonable values.

3.5 Influence of temperature on the mean amplitude of pressure fluctuations

The measurements of pressure drop fluctuations and differential pressure fluctuations were studied at

various temperatures. The mean amplitudes at these temperatures are shown in **Figs. 9, 10, 11** and **12**. From these figures, we find that the pressure amplitude is related to the temperature and (Uo/Umf) or $(Uo-Umf)$. At the same (Uo/Umf) or $(Uo-Umf)$, the pressure drop amplitude decreases as the temperature increases. This result is similar to the result of Svoboda *et al.*[18] Sadasivan *et al.*[15] found that the dimensionless pressure fluctuation amplitude is proportional to the bubble size to the 1.213 power:

$$\delta \propto Db^{1.213} \tag{8}$$

The decrease of amplitude at the elevated temperature can be considered as a decrease of bubble size. The same conclusion was obtained by Geldart and Kapoor,[8] Mii *et al.*,[13] and Stublington *et al.*[17] From Fig. 8, the effect of temperature on bubble rising velocity at the same $(Uo-Umf)$ is not so large. From Davidson and Harrison,[4] the bubble rising velocity is expressed as

$$Ub=(Uo-Umf)+k(gDb)^{1/2} \tag{9}$$

The temperature effect on the second term of Eq. 9 is not large. Although temperature has some effect on bubble size,[17] the overall effect of temperature on Ub is quite small. In the past, most pressure fluctuation studies were limited to pressure drop fluctuations, because they can be measured easily (only the probe location need be determined). Few measurements of the differential pressure fluctuations were obtained.[16] This method can be used to interpret the local bubble behavior or inhomogeneities in the bed, though the distance between two probes influences the values of measurements, and therefore different bubble sizes give different interpretations of signals. The local bubble behavior influenced by the temperature can therefore be evaluated from the differential pressure fluctuation signals, since it seems reasonable to correlate the fluctuation amplitude to the bubble size, as mentioned in the former part of this section. If the magnitude of pressure amplitude is related to a "gas bubble diameter" or to a characteristic dimension of inhomogeneity in a fluidized bed (as in the study by Sadasivan *et al.*[15]), the conclusion of decreasing gas bubble size at elevated temperature can be drawn.

3.6 Influence of temperature on the major frequency of pressure fluctuations

The frequency spectrum of pressure drop fluctuations can be interpreted as the frequency distribution of bubble eruption. The major frequencies at various temperatures for silica/air and alumina/air systems are shown in **Figs. 13** and **14** respectively. They increase considerably with increasing temperature. This behavior agrees with the fact from the two-phase theory [Tommy and Johnstone[19]] that for the same excess gas flow rate a small bubble has a higher bubble

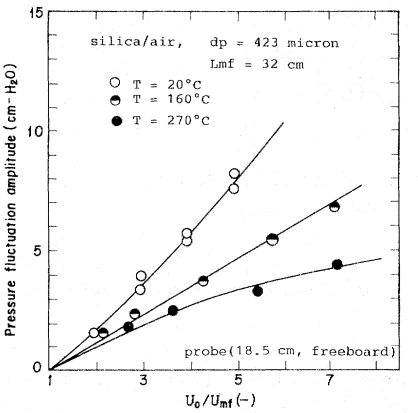

Fig. 9. Pressure drop fluctuations amplitude v.s. Uo at various temperatures for silica/air system

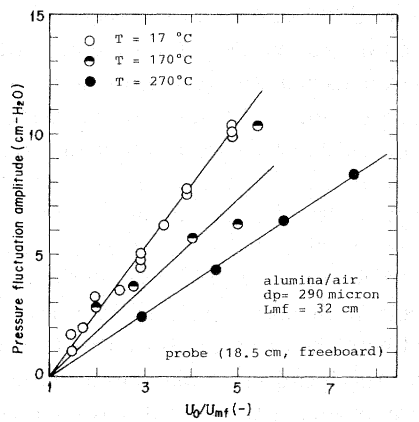

Fig. 10. Pressure drop fluctuations amplitude v.s. Uo/Umf at various temperatures for alumina/air system

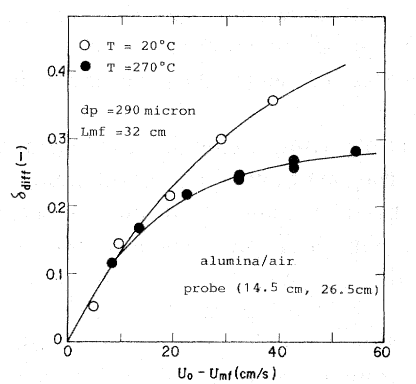

Fig. 11. Dimensionless differential pressure fluctuations amplitude v.s. Uo at various temperatures for alumina/air system

frequency, i.e. $f=(Uo-Umf)\times A/Vb$, the main reason being that bubble size decreases as the temperature increases.

From the standpoint of quality of fluidization, the influence of temperature on behavior is generally favorable. At elevated temperatures the regime of good aggregative fluidization becomes larger and the pressure fluctuations become smaller and more rapid

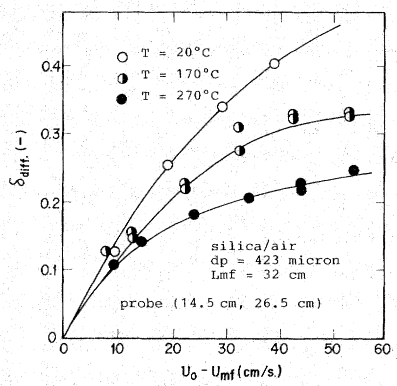

Fig. 12. Dimensionless differential pressure fluctuations amplitude v.s. *Uo* at various temperatures for silica/air system

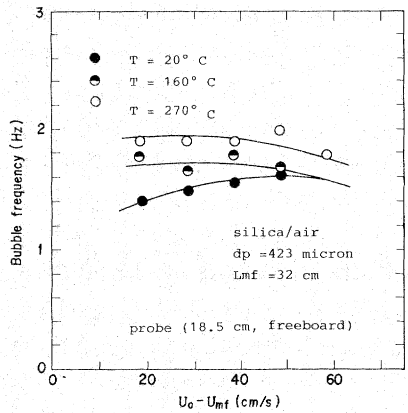

Fig. 13. Bubble eruption frequency v.s. *Uo* at various temperatures for silica/air system

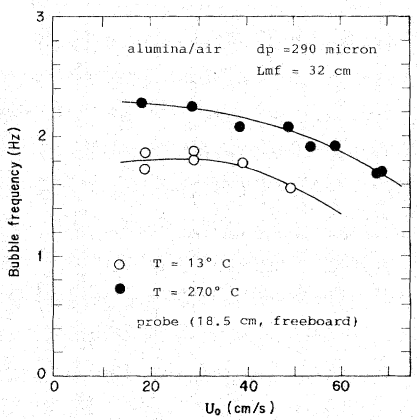

Fig. 14. Bubble eruption frequency v.s. *Uo* at various temperatures for alumina/air system

than at ambient temperature.[10,18]

Conclusions

The minimum fluidization velocity at elevated temperatures has been studied for group B particles. Two peaks of the p.d.f. of pressure drop fluctuations measured at the bed surface are observed at ambient temperature, but are not found at elevated temperatures at the same gas flow rate.

There is a maximum amplitude in the middle part of the fluidized bed at ambient temperature when silica particles are used. It is found that the maximum amplitude will shift with increasing temperature and gas flow rate.

At higher flow rate, bubble rising velocities are insignificantly affected by temperature change at the same excess gas velocity.

Mean amplitudes of pressure drop fluctuations, differential pressure fluctuations and major frequencies of bubble eruption depend considerably on both excess gas velocity and temperature. At elevated temperatures the mean amplitudes decrease and the major frequencies increase, implying a broad regime of good aggregative fluidization.

Acknowledgement

The authors are grateful to the National Science Council, R.O.C. for financial support.

Nomenclature

A	=	cross-sectional area	[m^2]
Db	=	bubble size	[m]
dp	=	particle diameter	[m]
f	=	frequency of pressure drop fluctuations	[Hz]
fd	=	major frequency	[Hz]
fs	=	side frequency	[Hz]
g	=	gravitational acceleration	[m/s^2]
$Gp(f)$	=	power spectral density function	[Pa/Hz]
hv	=	vertical distance from the distributor	[m]
k	=	constant	[—]
L	=	distance of location at points 1 and 2	[m]
P	=	pressure	[Pa]
$\overline{P}$	=	mean of pressure signals	[Pa]
$p.d.f.$	=	probability density function	[1/Pa]
Pi	=	pressure signal series	[Pa]
$P1$	=	pressure signals at point 1	[Pa]
$P2$	=	pressure signals at point 2	[Pa]
Re_{mf}	=	Reynolds number at *Umf*	[—]
$Rp(\tau)$	=	autocorrelation function with time lag τ	[Pa^2]
t	=	time	[s]
T	=	temperature	[K]
T_{max}	=	the time lag with maximum cross-correlation	[s]
Umf	=	minimum fluidization velocity	[m/s]
Uo	=	superficial velocity	[m/s]
Vb	=	bubble volume	[m^3]
Y	=	mean amplitude of pressure fluctuations	[Pa]
δ	=	dimensionless pressure fluctuation amplitude	[—]
δ_{diff}	=	dimensionless mean amplitude of differential pressure fluctuations	[—]
τ	=	time lag	[s]
τ_m	=	period	[s]
ϕ_{12}	=	cross-correlation function	[Pa2]

Literature Cited

1) Box, G. E. P. and G. M. Jenkins, "Time Series Analysis: Forecasting and Control," Rev. ed., Holden-Day, San

Francisco (1976).
2) Broadhurst, T. E. and H. A. Becker, in "Fluidization Technology" (D. L. Keairns, ed.), p. 63, vol. I, Hemisphere Pub. Corp., Washington (1976).
3) Cooley, J. W. and W. Turkey: *Math. Comp.*, **19**, 297 (1965).
4) Davidson, J. F. and D. Harrison, "Fluidized Particles", Cambridge Univ. Press, London (1963).
5) Fan, L. T., T. C. Ho, S. Hiraoka and W. P. Walawender: *AIChE J.*, **27**, 388 (1981).
6) Fan, L. T., T. C. Ho and W. P. Walawender: *AIChE J.*, **29**, 33 (1983).
7) Geldart, D.: *Powder Technol.*, **7**, 285 (1973).
8) Geldart, D. and D. S. Kapoor: *Chem. Eng. Sci.*, **31**, 842 (1976).
9) Kang, W. K., J. P. Sutherland and G. L. Osberg: *Ind. Eng. Chem. Fund.*, **6**, 499 (1967).
10) Kai, T. and S. Furusaki: *J. Chem. Eng. Japan*, **18**, 113 (1985).
11) Lan, C. W., "Pressure Fluctuation Measurement and its Application in the Scale-up of Gas-Solid Fluidized Bed," M. S. Thesis, Dept. of Chemical Engineering, National Taiwan University, Taipei, Taiwan (1986).
12) Lirag, R. C. and H. Littman: *AIChE. Symp. Ser.*, **67**, 11 (1971).
13) Mii, T., K. Yoshida and D. Kunii: *J. Chem. Eng. Japan*, **6**, 100 (1973).
14) Puncochar, M., J. Drahos, J. Cermak and K. Selucky: *Chem. Eng. Commu.*, **35**, 81 (1985).
15) Sadasivan, N., D. Barreteau, and C. Laguerie: *Powder Technol.*, **26**, 67 (1980).
16) Sitnai, O.: *Chem. Eng. Sci.*, **37**, 1059 (1982).
17) Stubington, J. F., D. Barrett and G. Lowry: *Chem. Eng. Res. Dev.*, **62**, 173 (1984).
18) Svoboda, K., J. Cermak, M. Hartman, J. Drahos and K. Selucky: *Ind. Eng. Chem. Proc. Des. Dev.*, **22**, 514 (1983).
19) Toomey, R. D. and H. F. Johnstone: *Chem. Eng. Prog.*, **48**, May, 220 (1952).
20) Wen, C. Y. and Y. H. Yu: *AIChE J.*, **12**, 610 (1966).
21) Winter, O.: *AIChE J.*, **14**, 426 (1968).